JOURNAL OF GEOPHYSICAL RESEARCH, VOL. 99, NO. B12, PAGES 23,939–23,950, DECEMBER 10, 1994

Atmospheric pressure loading effects on Global Positioning System coordinate determinations

Tonie M. vanDam
Geosciences Laboratory, NOAA, Silver Spring, Maryland

Geoffrey Blewitt
Department of Surveying, University of Newcastle upon Tyne, Newcastle upon Tyne, England

Michael B. Heflin
Jet Propulsion Laboratory, California Institute of Technology, Pasadena

Abstract. Earth deformation signals caused by atmospheric pressure loading are detected in vertical position estimates at Global Positioning System (GPS) stations. Surface displacements due to changes in atmospheric pressure account for up to 24% of the total variance in the GPS height estimates. The detected loading signals are larger at higher latitudes where pressure variations are greatest; the largest effect is observed at Fairbanks, Alaska (latitude 65°), with a signal RMS of 5 mm. Out of 19 continuously operating GPS sites (with a mean of 281 daily solutions per site), 18 show a positive correlation between the GPS vertical estimates and the modeled loading displacements. Accounting for loading reduces the variance of the vertical station positions on 12 of the 19 sites investigated. Removing the modeled pressure loading from GPS determinations of baseline length for baselines longer than 6000 km reduces the variance on 73 of the 117 baselines investigated. The slight increase in variance for some of the sites and baselines is consistent with expected statistical fluctuations. The results from most stations are consistent with ~65% of the modeled pressure load being found in the GPS vertical position measurements. Removing an annual signal from both the measured heights and the modeled load time series leaves this value unchanged. The source of the remaining discrepancy between the modeled and observed loading signal may be the result of (1) anisotropic effects in the Earth's loading response, (2) errors in GPS estimates of tropospheric delay, (3) errors in the surface pressure data, or (4) annual signals in the time series of loading and station heights. In addition, we find that using site dependent coefficients, determined by fitting local pressure to the modeled radial displacements, reduces the variance of the measured station heights as well as or better than using the global convolution sum.

Introduction

Recent advances in Global Positioning System (GPS) receiver hardware and data analysis software and techniques have allowed for the determination of weekly averaged vertical station positions with a precision of approximately 7 mm [*Blewitt et al.*, 1993] at the best determined sites. (The average over all sites is 15 mm.) This level of measurement precision is sufficient to meet the requirements of a few millimeters per year for (1) determining the nature of variations in land height that occur on global scales and at timescales of decades (e.g., postglacial rebound), and (2) tying global tide gauge measurements into a stable Earth-centered reference frame for determining sea level variations in an absolute rather than a relative sense.

Whatever the proposed application, interpretations of GPS measured changes in station positions need to assess the role of position changes due to loading phenomena. This is particularly important when the geodetic signal of interest is of the same order of magnitude as the amplitude of the loading signal itself. In this case, erroneous conclusions may be drawn with regard to the causes of station height variations. In this paper, we consider the effects of atmospheric pressure loading on precise GPS measurements.

We compare daily GPS geodetic positions with modeled estimates of atmospheric pressure loading for a time period of approximately 300 days. We only look at data from a representative subset of the 20-40 GPS stations typically used in a global solution. The pressure-induced vertical surface displacements are modeled by convolving *Farrell's* [1972] elastic Green's functions with global pressure data. Vertical displacements predicted using global pressure data are found to be significant in terms of the precision of GPS position determinations.

We assess the influence of the pressure loading effects on GPS station heights by comparing the weighted root-mean-square (WRMS) scatter of the height residuals about a secular trend before and after applying corrections for the pressure loading contribution. The data set contains station heights from 19 continuously operating GPS stations whose velocities are very well determined. We conclude that the atmospheric loading signal does contribute to the observed scatter in station heights at many of the stations investigated. We additionally compare GPS

Paper number 94JB02122.
0148-0227/94/94JB-02122$05.00

determined baseline length changes with predicted pressure loading effects. After correcting for the loading we observe a reduction in scatter on 62% of the baselines used in this analysis.

Numerical analyses [*Rabbel and Zschau*, 1985; *vanDam and Wahr*, 1987; *Manabe et al.*, 1991; *Rabble and Schuh*, 1986] have suggested that pressure loading can cause peak radial displacements of the Earth's surface as large as 10 to 25 mm with associated horizontal displacements of one-third to one-tenth this magnitude. The temporal variations of these modeled surface displacements are dominated by periods of approximately 2 weeks and are associated with the passage of synoptic scale (order 1000-2000 km) pressure systems.

Although the vertical motion is the largest component of the surface displacement associated with pressure loading, it is also the least well determined in geodetic analyses. For very long baseline interferometry (VLBI), the weighted root-mean-square (WRMS) of station height estimates is approximately 20 mm (T. Herring, personal communication, 1992), which is 3 times that of the horizontal coordinates and 4 times the RMS scatter predicted from pressure loading effects. As a result, reliably identifying the effects of atmospheric loading in VLBI estimates of vertical station positions is difficult [*Manabe et al.*, 1991; *MacMillan and Gipson,* 1994]. Direct analysis of loading induced vertical displacements is compromised in the case of VLBI because of polar motion and even larger UT1 variations. This is not a fundamental limitation of VLBI; rather it is related to the inability of any sparse geodetic network to distinguish between the daily motion of a few station positions and variations in Earth orientation. It is difficult for any geodetic network substantially smaller than the globe to distinguish a common vertical motion of all of the stations from a net translation of the entire network.

In the case of daily VLBI analyses, which typically include only a few operating stations on any given day, it is difficult to determine the variation in height for any individual station. VLBI is inherently a differential technique, so height variations appear in the chord distance ("baseline length") between sites that are far apart. However, VLBI measures not only distances but also orientation of the network with respect to distant quasars: hence it is also possible to look at variations in the vertical component of the vector between sites, even over short distances. The baseline vertical component, however, is not simply related to the station vertical component for very long baselines. Moreover, vector components are sensitive to errors in the determination of polar motion and UT1. Thus examination of the baseline length changes is the most straightforward way to look for the effect of atmospheric loading in VLBI data. In this way, *vanDam and Herring* [1994] detected statistically significant pressure loading effects, but the method inherently limits the ability to assess models for individual sites since the method determines the combined loading effect on both stations in each baseline.

In contrast to VLBI, a typical daily GPS network is composed of a global distribution of usually $n \approx 20$ to 40 stations (the number of continuously operating stations has increased with time since 1992). The resulting $n(n-1)/2$ baseline lengths and n geocentric radii (i.e., distances from the Earth's center of mass) can be used to construct a rigid closed polyhedron with a center of mass defined by the geocentric radii. (The $n(n-1)/2$ baseline lengths and n geocentric radii are not independent. However, all correlations are taken into account in the analysis.) Limited by mismodeling of nongravitational forces on the satellites, the location of the centroid of the polyhedron is uncertain at the decimeter level; as a result, the entire global network solution can be displaced at that level [*Blewitt et al.,* 1992; *Vigue et al.,* 1992]. However, if a global translation is removed from the daily solutions (by a procedure that will be described later), then individual station height variations at the few millimeter level can be determined from distortions in the shape of the polyhedron [*Blewitt et al.*, 1993]. The ambiguity as to which site is causing the distortion decreases as the number of stations increases. For example, in the absurd limit of a two-station network, there is no way to discriminate which station is moving. For a 40-station network, a single station's motion stands out with respect to the reference frame defined by the average position of all stations. The WRMS of daily GPS station height estimates is approximately 10 mm (this is in contrast to the 7 mm precision observed in the weekly determinations of vertical station positions). We estimate that "reference frame noise," caused by the finite number of stations, contributes less than 2 mm random errors in the heights. This noise is small compared to atmospheric loading signals and individual station height errors.

Finally, the vertical motions of interest in this paper have horizontal scale lengths of order 1000 km which is comparable to the typical spacing of GPS networks. Therefore GPS is well designed for determining motions of the sort expected from week to week surface pressure variations. The following analysis demonstrates that it is feasible to discern the pressure loading signal in station height residuals determined from a global GPS network solution.

Data and Analysis

GPS Data Reduction

Values of GPS station heights were determined using the no-fiducial approach [*Heflin et al.*, 1992]. The analysis was carried out with the GIPSY (GPS Inferred Positioning SYstem) software system developed at the Jet Propulsion Laboratory [*Lichten and Border*, 1987; *Sovers and Border*, 1990]. The procedure follows that described by *Heflin et al.* [1992] except for the details as follows: (1) Polar motion bias and the rate of UT1-UTC were estimated daily. (2) The *Sovers and Border* [1990] solid Earth tide model was used along with a standard pole tide model; no ocean loading model was applied. (3) We modeled the GPS satellite motion as a nine-parameter epoch state vector which included three-dimensional position, velocity, and solar radiation. The noise model for this variation is Gauss Markov with a 4-hour time constant and 10% a priori standard deviation. During periods when a satellite is in the Earth's shadow, the extra variation allows significantly better modeling of the satellite's motion [*Vigue et al.*, 1993; *Zumberge et al.*, 1993].

Station Height and Baseline Length Time Series

Briefly, the height estimates are derived by first fitting all the data to a constant station three-dimensional velocity model, and then deriving the height residual to that estimated model for each day in question. The actual steps to obtain our time series of daily station height estimates are summarized as follows.

1. Reduce the GPS data independently each day as described above, saving the estimates and covariance matrix for the Cartesian coordinates of all stations and applying loose a priori constraints (10 m). We call these the " daily free solutions."

2. Perform a weighted least squares fit of all these daily free solutions to a kinematic model of station motion. The station parameters include a three-dimensional epoch position plus a three-dimensional velocity vector; but a few stations require additional epoch coordinates to account for seismic displacement or antenna relocation (however, preseismic and postseismic velocity is constrained to be equal). We call this the "free kinematic solution."

3. Align the daily free kinematic solutions with the International Terrestrial Reference Frame (ITRF) [International Earth Rotation Service (IERS), 1993]. First, account for secular crustal motion by applying tight velocity constraints (0.1 mm/yr) for those stations listed in the ITRF. (We do not constrain the station velocities to ITRF values; only the net rotation, translation, and scale rate are constrained to match ITRF values.) Following the method of *Blewitt et al.* [1992], apply a projection operator to the covariance matrix of the combined solution to remove components of formal error that are correlated with reference frame orientation, origin, and scale. Then, minimizing the weighted least squares coordinate differences, transform the coordinates of the kinematic solution into the ITRF, applying three estimated rotations, three translations, and one scale factor. The scale (and scale rate) does not in principle require constraints and are intrinsically very well defined by fixing the speed of light and GM. We call this the "transformed kinematic solution." This is the reference solution against which height variations will be gauged.

4. Using the (constrained) velocity field, map the transformed kinematic solution to the date of each daily solution. We call these the "mapped solutions."

5. Align each of the daily solutions with the mapped solutions. First, apply a projection operator to the covariance matrix of each daily solution to remove frame-correlated errors. Then, minimizing the weighted least squares coordinate differences, transform each daily solution into the mapped solution, applying three estimated rotations, three translations, and one scale factor. We call these the "daily transformed solutions."

6. For each day, compute the difference in ellipsoidal station heights between the daily transformed solution and the mapped solution. Note that the specific choice of reference frame and ellipsoid definition is inconsequential for our purposes, because we are only interested in height variations, which are no larger than a few centimeters, and are thus insensitive to the definition of the local vertical direction.

Station heights from 19 GPS stations (listed in Table 1 and shown in Figure 1) were used in this analysis. We restricted the analysis to include only those stations having formal errors on their velocity of less than 5 mm/yr. We impose this constraint to try (1) to ensure a long time span for our analysis and (2) to enhance the signal to noise ratio in our sample of stations. The formal error restriction essentially limits the global coverage of the subset of stations to the northern hemisphere. The larger formal errors observed in data from the southern hemisphere are probably due to the poor geographic coverage of stations there. Sparse coverage may contribute to large formal errors in two possible ways: (1) Lack of observations, especially where there is a lack of common visibility of the same satellites for distant stations. (2) The denser northern hemisphere dominates the definition of the reference frame which is based on linear combinations of all the station coordinates. Therefore the northern hemisphere is heavily weighted in the frame definition. In the limit that the northern hemisphere completely dominates the frame definition, there is a long lever arm to the southern hemisphere which allows those stations to vary more (in a regionally correlated way) from day to day.

The number of observations at each site (Table 1) is highly

Table 1. Weighted Variances for Parameters of Interest

Station[a]	Latitude, deg	Number of Data Points	Distance From Coast, km	Heights, mm^2	Loading, mm^2	Corrected Heights, mm^2	Variance Change, mm^2
Ny-Alesund (2)	78.92	242	< 100	286.71	10.15	276.73	-9.97 ± 6.82
Tromso (1)	69.67	310	< 100	122.75	18.85	101.21	-21.54 ± 5.00
Fairbanks (1)	64.97	304	500	203.68	24.09	154.73	-48.95 ± 7.29
Yellowknife (2)	62.47	320	1500	75.45	21.69	66.05	-9.41 ± 4.04
Metsahovi (2)	60.22	302	< 100	90.08	25.08	81.67	-8.41 ± 4.94
Onsala (3)	57.38	301	< 100	85.92	13.81	95.00	9.08 ± 3.92
Kootwijk (2)	52.17	307	110	51.27	14.74	50.96	-0.31 ± 2.90
Herstmonceux (3)	50.87	237	< 100	45.15	9.60	53.47	8.32 ± 2.69
Penticton (2)	49.32	306	400	54.96	6.82	53.92	-1.05 ± 2.14
Wettzell (2)	49.13	296	600	67.27	13.89	63.97	-3.30 ± 3.32
Alberthead (3)	48.38	319	< 100	62.35	4.77	65.16	2.81 ± 1.92
St. John's (3)	47.60	306	< 100	106.72	5.00	109.19	2.47 ± 2.63
Algonquin (2)	45.95	315	1000	78.19	10.01	70.57	-7.62 ± 2.97
Matera (3)	40.63	294	< 100	97.11	6.86	99.32	2.21 ± 2.98
Madrid (3)	40.42	320	400	108.04	5.36	111.12	3.09 ± 2.68
Goldstone (1)	35.23	281	150	110.71	2.25	106.94	-3.77 ± 1.86
JPLM (2)	34.20	255	< 100	84.09	1.88	83.56	-0.52 ± 1.57
Pinyon Flats (1)	33.60	83	< 100	156.81	0.75	152.26	-4.55 ± 2.38
Kokee (3)	22.17	251	< 100	388.69	0.33	389.14	0.46 ± 1.44

Variances in millimeters squared of the GPS vertical station measurements, of the atmospheric loading signal, of the corrected station position measurements, and of the observed variance change.

[a]The locations of the GPS stations are: Ny-Alesund, Norway; Tromso, Norway; Fairbanks, Alaska; Yellowknife, Northwest Territories, Canada ; Metsahovi, Finland; Onsala, Sweden; Kootwijk, Apeldoorn, Netherlands; Herstmonceux, East Sussex, England; Penticton, Canada; Wettzell, Germany; Alberthead, British Columbia, Canada; St. John's, Newfoundland, Canada; Algonquin, Ontario, Canada; Matera, Italy; Madrid, Spain; Goldstone, California; Pasadena, California; Pinyon Flats, California; Kokee Park, Kauai, Hawaii. The numbers following the station names indicate how the variance changed at that station once the corrections for atmospheric pressure loading were applied: (1) stations where a greater than expected change in variance was observed; (2) stations where a less than expected variance reduction was observed; (3) stations where an increase in variance was observed.

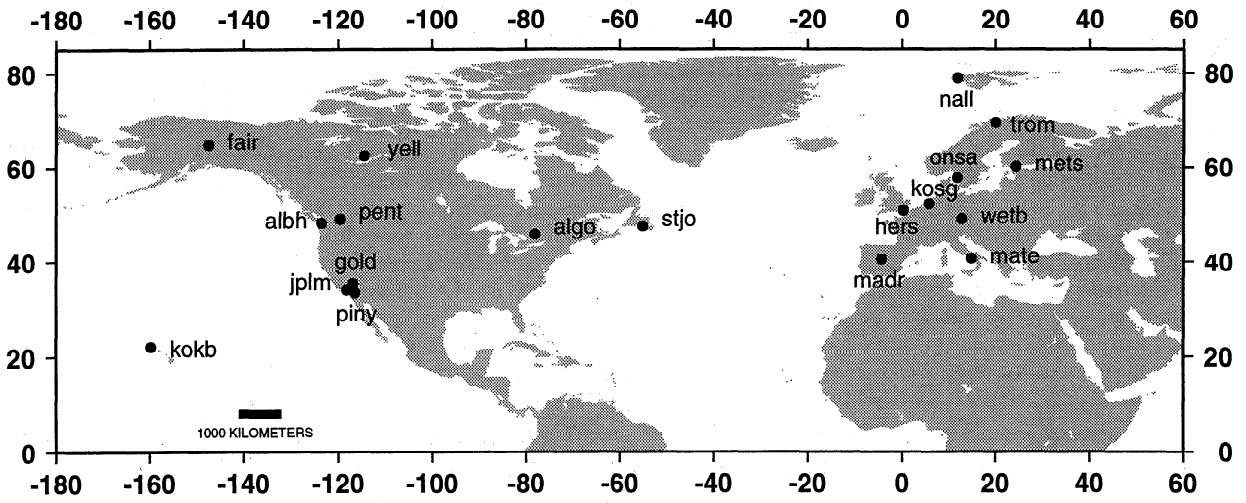

Figure 1. Continuously operating GPS stations used in this analysis and their geographic distribution. Note that most stations are located within 500 kilometers of the nearest coastline.

variable and is dependent upon when the station became operational and that station's equipment reliability. The data span the time period from June 1992 to September, 1993.

We also analyzed 117 GPS baseline lengths. The baselines were restricted to those measured more than 100 times and longer than 6000 kilometers in length.

Atmospheric Loading Effects

The effects of atmospheric pressure loading are computed by convolving Farrell's elastic Green's functions with twice daily global surface pressure values (2.5° x 2.5° grid) estimated by the National Meteorological Center (NMC) and archived by the National Center for Atmospheric Research (NCAR). The NMC surface pressure grids are derived from a Global Objective Analysis (GANL). The GANL takes as input surface measurements of pressure, wind, and moisture reported by ships, buoys and meteorological stations, rawinsonde measurements, and satellite measurements of sea surface temperatures. The data set is most accurate over North America and Europe and is weakest over most of Asia, the former Soviet Union and the Indian subcontinent (S. Lord, personal communication, 1994). In addition, the absence of surface meteorological data over the oceans reduces the data set's reliability here as well. Since we are using "surface" pressure values; variations in pressure due to the effects of surface topography are already taken care of. Details of the technique used to model the loading effects are provided by *vanDam and Wahr* [1987] or *vanDam and Herring* [1994] and will not be reproduced here.

Surface displacements are calculated using an Earth model in which the oceans respond as a modified inverted barometer to atmospheric pressure loading. A pure inverted barometer response is defined such that for every millibar increase in pressure the ocean surface compensates by depressing a centimeter. In this case, the total combined mass of air and water over a particular area remains constant, and thus there is no pressure change at the ocean floor from changing atmospheric pressure. If, however, we impose the constraint that oceanic mass is conserved, then a net increase or decrease in the total mass of air above the oceans would produce a uniform pressure, acting everywhere on the Earth's surface under the oceans and equal to

$$D = \frac{\int_A \Delta P dS}{A} \quad (1)$$

where ΔP is the local change in pressure, A is the surface area of the oceans, and the integral is taken over the ocean surface [*vanDam and Wahr,* 1987].

Island sites and those located on a coastline respond differently than inland sites to the same pressure forcing. Since pressure highs and lows are correlated over distances of hundreds of kilometers, sites within this distance of the coast will respond differently than inland sites to the same pressure forcing due to the inverted barometer response of the ocean. For a perfect inverted barometer response, a station on the coastline will feel only about 50% of the total effect of a regional-scale pressure variation centered at the station, whereas a station 1000 km inland will not be sensitive to the oceanic response. (The pressure response at coastal stations is actually significantly more complicated than the idealized example just presented. The shape of the coastline, the correlation between wind stress and pressure there, and the geometry and depth of the continental shelf as well as wind-driven shore currents complicate the oceanic response to pressure significantly so that few tide gauges actually observe an exact inverted barometer response to pressure. See *Chelton and Enfield* [1986] for a summary of observational evidence for the inverted barometer response.) In this paper, we will simply define a "coastal station" to be a site located less than 500 km from the coast (see Table 1). Using this definition most of the sites used in this analysis are considered coastal sites. Only Fairbanks, Yellowknife, Algonquin, and Wettzell would classify as inland sites.

Results

Modeled radial displacements for six characteristic sites (Yellowknife, Canada; Tromso, Norway; Wettzell, Germany; St. John's, Newfoundland, Canada; Pasadena, California (JPLM); and Kauai, Hawaii (Kokee)) are represented by the dashed lines in Figure 2 (the solid lines in Figure 2 are GPS residuals of the vertical station positions to be discussed below). Please note that the vertical scale is different for the results at Kokee. For visual clarity only, the data were smoothed using a five-point moving average. No smoothing was applied to the data used in the calculations or statistics in this paper. The modeled

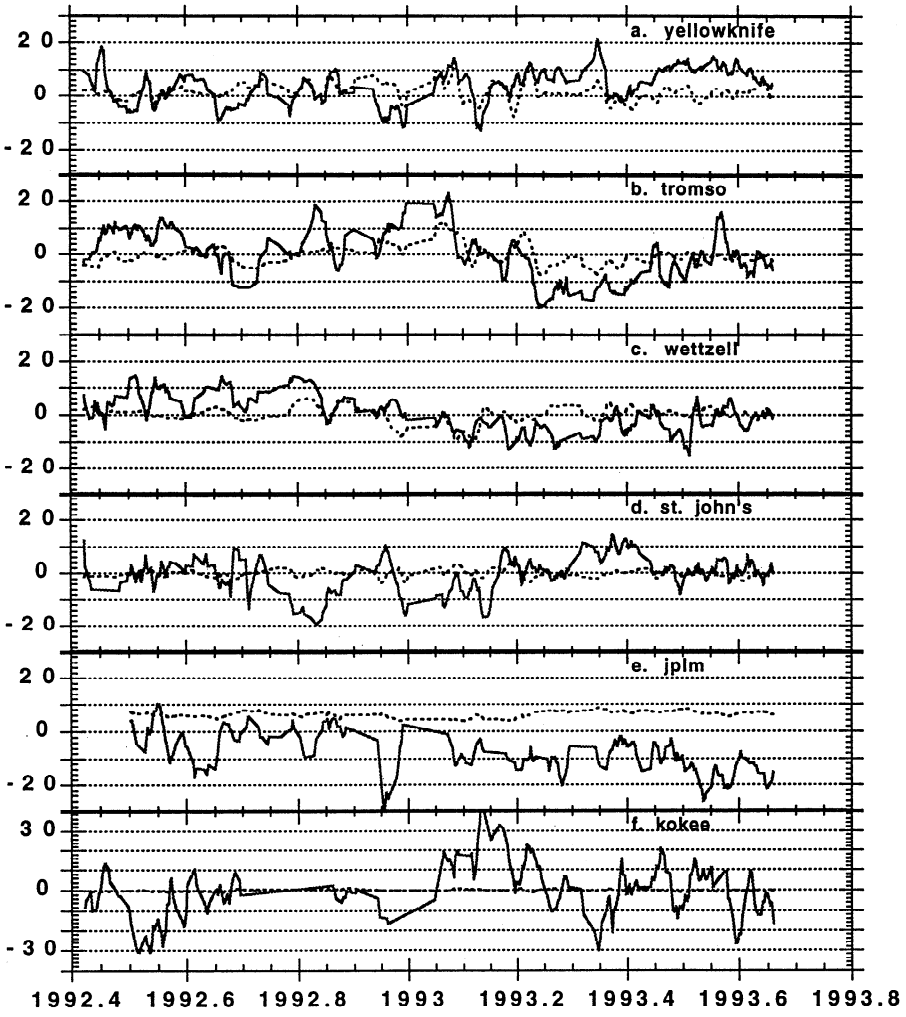

Figure 2. GPS vertical position measurements (solid line) and corresponding estimates of atmospheric pressure loading (dashed line) both in millimeters. (a) Yellowknife, Northwest Territories, Canada (b) Tromso, Norway (c) Wettzell, Germany, (d) St. John's, Newfoundland, (e) Pasadena, California (JPLM), and (f) Kokee, Hawaii. Note that the vertical scale for the Kokee data differs from that of the other stations. Data have been smoothed using a five-point moving average.

displacements at Wettzell (Figure 2c) are typical of noncoastal midlatitude sites. The largest variations (peak-to-peak) in the radial displacements are of the order of 15 mm and occur on timescales of 1-2 weeks. For comparison, predicted surface displacements at St. John's are shown in Figure 2d. Despite lying at approximately the same latitude as Wettzell, the magnitude of the estimated loading signals are smaller here because of St. John's proximity to the Atlantic Ocean.

At higher latitudes, the loading effects are systematically larger due to the larger storms found there. Surface displacements at Yellowknife, for example (Figure 2a), are even larger than those at Wettzell. A slight reduction in the magnitude of the loading is observed Tromso (Figure 2b), a coastal site at the same latitude as Yellowknife.

Most continuously operating GPS sites within 35° of the equator are either coastal or island sites. The influence of atmospheric loading at these sites is probably very typical to what we observe at JPLM (Figure 2e) and Kokee (Figure 2f). The small loading signal at these sites is very small due to the small pressure variations found at these latitudes.

The variances of the predicted loading displacements for all sites investigated in this paper vary between 0 and 25 mm^2 (see Table 1). The largest values are associated with inland stations in the mid-latitudes to high-latitudes, the smallest with low-latitude coastal sites. In contrast, the variance of the observed GPS station height residuals varies between 45 and 390 mm^2 (Table 1). Therefore we would expect the loading signal to contribute only slightly to the statistics of the station height residuals.

GPS measured height variations for the six sites are represented by the solid lines in Figure 2. Juxtaposing the two time series reveals the degree to which the GPS residuals track temporal variations in atmospheric pressure loading (this is true to a lesser extent at JPLM and Kokee). More importantly though, Figure 2 demonstrates that GPS is sensitive to atmospheric loading as an error source. The correlation between the predicted and observed signals is given in Table 2. The values indicate that

Table 2. Scale Factor (Ratio of Modeled to Observed Height Variations) and Correlation Coefficient Between GPS Station Height Residuals and Modeled Loading Effects

Station	Scaling Factor[a]	Correlation Coefficient	Expected Correlation
Ny-Alesund	0.49 ± .02	0.19 ± 0.06	0.19
Tromso[b]	1.02 ± .01	0.42 ± 0.05	0.39
Fairbanks[b]	1.44 ± .01	0.52 ± 0.05	0.34
Yellowknife[b]	0.66 ± .01	0.38 ± 0.05	0.54
Metsahovi[b]	0.63 ± .01	0.35 ± 0.05	0.53
Onsala	0.21 ± .02	0.07 ± 0.06	0.40
Kootwijk[b]	0.51 ± .02	0.27 ± 0.06	0.54
Herstmonceux	0.04 ± .02	0.03 ± 0.07	0.46
Penticton[b]	0.63 ± .02	0.20 ± 0.06	0.35
Wettzell[b]	0.55 ± .02	0.28 ± 0.06	0.45
Alberthead	0.15 ± .03	0.06 ± 0.06	0.28
St. John's	0.17 ± .03	0.05 ± 0.06	0.22
Algonquin[b]	0.93 ± .02	0.32 ± 0.05	0.36
Matera	0.28 ± .02	0.09 ± 0.06	0.27
Madrid	0.00 ± .03	0.05 ± 0.06	0.22
Goldstone[b]	1.26 ± .04	0.19 ± 0.06	0.14
JPLM	0.09 ± .05	0.10 ± 0.06	0.15
Pinyon Flats[b]	3.52 ± .13	0.24 ± 0.11	0.07
Kokee	-0.64 ± .11	-0.01 ± 0.06	0.03

[a]Scale factor is the weighted fit of modeled to observed station heights.

[b]Stations where modeled and observed height variations are correlated at the 99% confidence level.

the two time series are statistically correlated. The null hypothesis (zero correlation) can be rejected with a 0.02 level of significance for 10 of the 19 stations (indicated by a superscript b in Table 2). Table 2 also shows the correlation that would be expected if the predicted signal had no errors. The signals are weakly anticorrelated (-0.01 ± 0.06) for the station Kokee; however, this is consistent with the expected correlation of 0.03. The expected correlation for Kokee is so low because of the small pressure loading effects that would be predicted for a remote, low-latitude island site, assuming an inverted barometer response of the ocean.

Another feature of Figure 2 is the discrepancy between the amplitudes of the two signals. For example, the largest modeled surface displacements at Yellowknife and Wettzell (Figures 2a and 2c) appear to be only about half the magnitude of the GPS station height variations. A linear regression of the observed verticals with the modeled loading effects demonstrates that the best fit line through the data has a slope (scale factor) of between 0.5 and 1.5 for the sites exhibiting a strong correlation between the two signals (these sites are marked with a superscript b in Table 2). The scale factors at the sites with the weaker correlations are closer to 0.2 and are even negative at Kokee. The ratios of the modeled to observed station heights are shown in Figure 3 for all the sites. These results indicate that the GPS height variations are, in general, larger than the height variations predicted from the atmospheric loading model. This discrepancy could arise from either pressure-correlated errors in the GPS height determinations or from errors in modeling the loading effects. We discuss the possible error sources in detail later in the paper.

Statistical Analysis

There are a number of different techniques which could be used to assess the presence of the loading signals in the measured station heights. We have chosen to compare the variance of the height residuals before and after applying the corrections for the loading signals. However, variance calculations provide only estimates of the standard deviation of the observed quantities. These estimates are affected by noise in the measurements.

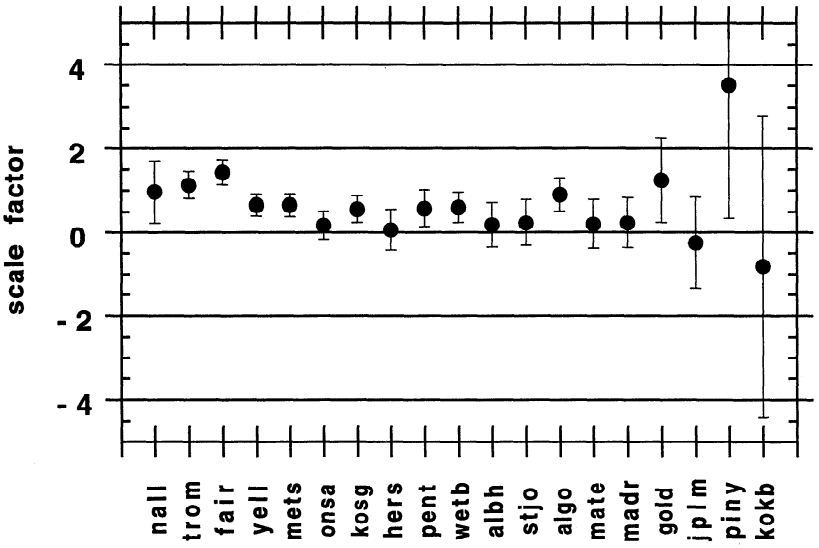

Figure 3. Plot of ratio of modeled to observed station height deviations. The station codes are NALL, Ny-Alesund, Norway; TROM, Tromso, Norway; FAIR, Fairbanks, Alaska; YELL, Yellowknife, Northwest Territories, Canada ; METS, Metsahovi, Finland; ONSA, Onsala Sweden; KOSG, Apeldoorn, Netherlands; HERS, East Sussex, England; PENT, Penticton, Canada; WETB, Wettzell, Germany; ALBH, Alberthead, British Columbia, Canada; STJO, St. John's, Newfoundland, Canada; ALGO, Algonquin, Ontario, Canada; MATE, Matera, Italy; MADR, Madrid, Spain; GOLD, Goldstone, California; JPLM, Pasadena, California; PINY, Pinyon Flats, California; KOKB, Kokee Park, Kauai, Hawaii. In general, the GPS station height residuals are about twice as large as the modeled loading effects.

VanDam and Herring [1994] derive the statistical properties of the changes in the variances of the height measurements when the loading corrections are applied. They assume that the pressure loading correction consists of both a true loading component, σ_l^2, and a fraction that represents noise, σ_l^2. The main results from derivations in their paper are

$$\left\langle \hat{\sigma}_{\delta b}^2 - \hat{\sigma}_{\delta c}^2 \right\rangle = \sigma_l^2 - \sigma_w^2 \quad (2)$$

$$\mathrm{var}(\hat{\sigma}_{\delta b}^2 - \hat{\sigma}_{\delta c}^2) = 4\sigma_v^2(\sigma_l^2 + \sigma_w^2)/(N-1) \quad (3)$$

(their equations (A10) and (A12)). Equation (2) gives the expectation of the change in the variance estimate of the station heights before, $\hat{\sigma}_{\delta b}^2$, and after, $\hat{\sigma}_{\delta c}^2$, applying the loading corrections in terms of the variance of the signal and the noise in the loading correction. Equation (1) gives the variance of the difference of the variance estimates when the variances are computed using finite numbers of measurements. Estimates for the formal errors associated with the NMC pressure data are not available. In order to treat each series of data in the same fashion, we weight the pressure data by the weight of the corresponding GPS measurement. The summaries of the computed statistical quantities are given in Tables 1, 3, and 4.

In Table 1, we give the values for the variance estimates of the height measurements before and after applying the loading corrections, the variance of the loading corrections themselves, and the change in the variance estimates along with the statistical uncertainty of the estimate of the change (equation (3)). In general, for the 12 sites where a reduction in RMS is observed, the pressure loading accounts for about 1-24% of the variance in the GPS residuals. If the load signal were noise free and the variance estimates were computed with infinite degrees of freedom, then the difference in the variance estimates before and after applying the loading correction would equal the variance of the load itself. However, in practice, this is not the case due to noise in the loading correction and because the statistics are computed with finite degrees of freedom. The results in Table 1 fall into three categories characterized by the change in variance when the load corrections are applied: (1) variance reduction greater than would be expected given the magnitude of the loading contribution; (2) variance reduction less than would be expected given the magnitude of the load contributions; and (3) variance increase when the load correction is applied. Stations in each category are indicated by the corresponding number.

Table 3. Statistical Expectations for Alternate Hypotheses

Station	Variance Reduction Less Than Observed (No Noise), %	Variance Reduction Greater Than Observed (No Signal), %
Tromso (1)	70.41	0.00
Fairbanks (1)	99.97	0.00
Goldstone (1)	79.29	0.06
Pinyon Flats (1)	94.45	1.30
Ny-Alesund (2)	48.97	0.16
Yellowknife (2)	0.12	0.00
Metsahovi (2)	0.04	0.00
Kootwijk (2)	0.00	0.00
Penticton (2)	0.34	0.01
Wettzell (2)	0.07	0.00
Algonquin (2)	21.11	0.00
JPLM (2)	19.35	6.25
Onsala (3)	0.00	11.41
Herstmonceux (3)	0.00	31.69
Alberthead (3)	0.00	15.41
St. John's (3)	0.22	16.77
Matera (3)	0.12	5.94
Madrid (3)	0.08	19.78
Kokee (3)	29.14	46.54

Statistics derived from data inversion (see text). Stations grouped according to category (explanation of categories of station names is given in Table 1). The probability of observing (1) a smaller reduction in the variance than that measured for the case of no noise in the pressure data is given in column 2 and (2) the probability of observing a greater reduction in the variance than measured for the case of no signal in the pressure data is given in column 3. Station codes given in the footnotes to Table 1.

Table 4. Statistical Expectations Derived from Data Inversion

Station	GPS Noise, mm^2	Loading Signal, mm^2	Loading Noise, mm^2	SNR of Loading
Tromso (1)	102.56	20.20	-1.34	-15.06
Fairbanks (1)	167.16	36.52	-12.43	-2.94
Goldstone (1)	154.15	2.65	-1.90	-1.40
Pinyon Flats (1)	107.70	3.01	-0.76	-3.96
Ny-Alesund (2)	276.65	10.06	0.09	113.80
Yellowknife (2)	59.91	15.55	6.14	2.53
Metsahovi (2)	73.34	16.75	8.33	2.01
Kootwijk (2)	43.75	7.53	7.21	1.04
Penticton (2)	51.03	3.93	2.89	1.36
Wettzell (2)	58.67	8.60	5.29	1.62
Algonquin (2)	69.37	8.81	1.19	7.38
JPLM (2)	82.89	1.20	0.68	1.77
Onsala(3)	83.55	2.36	11.44	0.21
Herstmonceux (3)	44.51	0.64	8.96	0.07
Alberthead (3)	61.37	0.98	3.79	0.26
St. John's (3)	105.45	1.27	3.74	0.34
Matera (3)	94.79	2.32	4.53	0.51
Madrid (3)	106.90	1.14	4.22	0.27
Kokee (3)	388.75	-0.06	0.40	-0.16

Statistics derived from data inversion (see text), GPS noise, pressure loading signal, pressure loading noise, signal to noise ratio of the loading. A negative value for loading noise indicates that more improvement was observed than would be expected given the magnitude of the loading. This phenomenon could occur due to random noise effects in the computation of the variances or if the noise in the load signal were correlated with GPS vertical measurement errors.

In Table 3, we quantify the effects of finite degrees of freedom by calculating the probabilities that (1) the variance improvement would have been less than observed if the load contribution were all signal, and (2) the variance improvement would have been greater than observed if the load contribution were all noise. The results indicate that for stations in category 1 there is a small probability that the observed variance reductions could be due to random noise. For these stations, the probability of seeing even greater improvements than those observed is between 1 and 30%.

For the stations in category 2 (excluding Ny-Alesund), there is a low probability (0-20%) that the observed improvement was less than expected due to random noise. In addition, there is a very small probability (~0 - 6%) that for stations in either category 1 or 2 a greater reduction would be observed if the loading estimates were all noise. For sites where an increase in the variance is observed, the results are consistent with the assumption of no signal in the load contribution at all. However, the statistics are also consistent with no noise as well, indicating that the GPS residuals do not have enough sensitivity to detect the presence of the loading contribution. Excluding Madrid, these sites are all located within 50 km of the nearest shoreline, pointing to the possibility that the atmospheric loading at the land/ocean boundary is being modeled incorrectly.

Estimates of the noise content in the GPS height residuals and in the loading time series can be obtained by inverting the variance changes [see *vanDam and Herring,* 1994]. Values of these quantities are given in Table 4 along with estimates of the ratio of the signal power to noise power in the loading contribution. The negative values of the loading noise variance are associated with stations where there was more reduction of the station height than expected. Since the variances are estimated variances, with associated noise due to finite degrees of freedom in their calculation, it is possible for the estimates to be negative although this is physically impossible. Negative noise values can be interpreted as either (1) random or systematic correlation between GPS height error and pressure, or (2) evidence that the signal is actually larger than that modeled. The expected level of random correlation is indicated by the standard errors given in Table 2.

In Figure 4, we plot the estimated load signal determined from the inversion (column 3, Table 4) against the total variance of the load (column 6, Table 1). A linear regression through these results (solid line) indicates that about 68.4% (± 10%) of the power in the modeled load correction is observed signal (i.e., is present in the GPS height residuals). The dashed line, included for comparison, has a slope of 1.

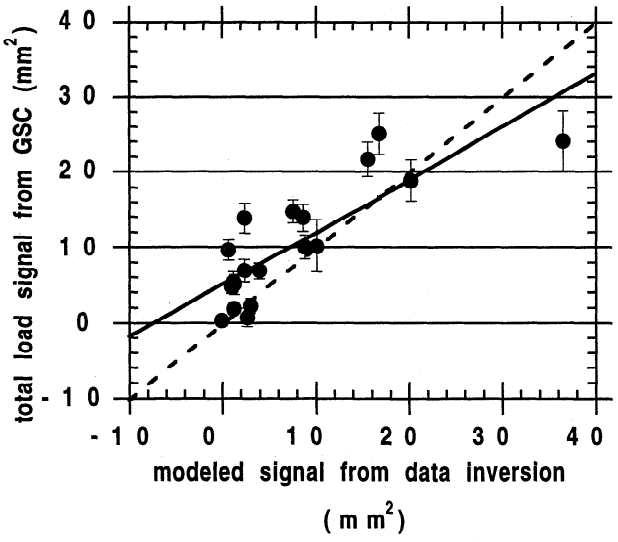

Figure 4. Plot of estimated pressure signal versus modeled pressure signals for all the stations investigated in this paper. The weighted fit (solid line) has a slope of 0.68, indicating that approximately 68% of the pressure signal is found in the GPS estimates of vertical station positions; the dashed line, included for reference, has a slope of 1.

Discussion

There are several reasons why correcting for the modeled load contribution does not reduce the scatter of the GPS station height residuals by the expected amount. These include noise in the NMC pressure data, failure of the inverted barometer at the relatively high temporal frequencies dominating the pressure variations, deficiencies in *Farrell's* [1972] Green's functions, and noise in the GPS station height residuals. The relative importance of each of these contributions is not clear at this time, although we have investigated the possible effects of some of these error sources.

The mismodeling of the loading effects due to assuming an inverted barometer response of the oceans was tested by recomputing the variance estimates for the stations under the assumption of a solid earth (i.e., no oceans). For Fairbanks, JPLM, and Pinyon Flats, California, the variance of the station heights is reduced even further (~1%) than when the predicted loading estimates were calculated using the inverted barometer ocean model. At the remaining sites, removing the oceans from the Earth model degrades the results. More precisely, stations where a variance reduction was observed showed less improvement than in the inverted barometer case; stations where there was an increase in the variance displayed even greater increases. These results indicate that at these sites an inverted barometer ocean response fits the GPS data better than does a "no oceans" Earth model. This comparison does not evaluate the effect of a more complex ocean/atmosphere interaction at the coastal sites. Additional sources of error at coastal stations that will also affect GPS station heights include ocean bottom pressure changes induced by wind stress or atmospheric pressure [see *Eubanks*, 1993] and wind-driven onshore loading.

We also examined the possibility that some of the undetected power in the loading predictions arises from underestimating the magnitude of the loading effects. Mismodeling of the loading values can result from either (1) deficiencies in *Farrell's* [1972] Green's functions or (2) inaccuracies in the NMC estimates of surface pressure. To verify the accuracy of the Green's functions, we recomputed the loading predictions using the Green's functions of *Pagiatakis* [1990]. The main feature of the Earth model used by Pagiatakis is that it includes anisotropy. The variance of the pressure loading effect increases by 3-4% (depending on the station) when the new Green's functions are used. Removing the new pressure loading effects from the GPS station height residuals does not significantly reduce the variance of the height residuals over the case when *Farrell's* [1972] Green's functions are used. The variances are reduced at five stations: Ny-Alesund, Tromso, Fairbanks, Goldstone, and Pinyon Flats by between 2 and 0.1%. Given that the differences between the Farrell and Pagiatakis loading signals are small, the additional reduction in the variances of the GPS station heights may be significant and may indicate that GPS station heights are sensitive to anisotropic effects in the Earth's loading response at these sites. The variance of the station heights increases slightly at the remaining 14 sites.

Unfortunately, this comparison does not really test for inaccuracies of the Green's functions since both sets of functions were derived using the same basic physics. However, the fact that we can essentially reproduce the results with two different sets of values points out that the loading corrections are at least of the correct order of magnitude. And given the fact that the loading needs to be geographically extensive (~ 1000 km), it is unlikely that the Earth models would be in error at this scale. Based on this reasoning, variations in the loading response due to

regional geology (i.e., we might expect a larger loading response at sites located on alluvium versus a site located on solid igneous or metamorphic rock) will only be important if the formations extend over regions and depths of 1000 km or greater. There are some continuously operating GPS sites (for example, the station at Richmond, Florida) that do meet this requirement, but because these sites did not satisfy the velocity formal error cutoff, they were not included in this analysis.

Another potential problem with the loading model may be the NMC values used to predict the loading effects. The NMC data may not adequately represent the actual surface pressure field because it is a smoothed (in space and in time) version of the real surface pressure field (K. Trenberth, personal communication, 1994). A comparison of 204 days of surface pressure recorded by the VLBI station at Fairbanks with NMC estimates of the pressure there indicates that while the RMS of the two time series is essentially the same (~10 mbar), individual estimates of local pressure typically disagree by 10 mbar. Maximum variations of as much as 35 mbar are also observed. If these 35-mbar discrepancies extend over a significant geographic region (> 500 km) and do not simply represent local pressure anomalies, then errors in the NMC data could account for some of the disagreement between the predicted loading effects and those actually observed in the GPS data. However, since there are only a relatively few meteorological stations within 500 km of Fairbanks, it would be difficult to determine if the pressure discrepancies were spatially coherent.

There is a larger distribution of meteorological stations in other parts of North American and in western Europe. We looked at surface pressure data collected by 350 meteorological stations located within 500 km of Wettzell for the month of January 1993. We compared the NMC local pressure with the local pressure reported by the meteorological station closest to Wettzell and found that the two time series were always in agreement to within 10 mbar. The better agreement between the two pressure series at Wettzell is due to the fact that there are more meteorological stations in western Europe than near Fairbanks, Alaska. The ability of the NMC data to reproduce local surface pressure appears to be geographically dependent. Stations in North America and western Europe are less likely to be affected by errors in the pressure than are stations elsewhere.

We compare the ability of the two pressure data sets to remove the pressure loading signal from the GPS height residuals. The local data are averaged into 2.5° x 2.5° bins to generate a global pressure grid similar to that produced by the NMC. When we remove this predicted loading signal from the GPS station heights, we find that for this one month of data the NMC data set reduces the scatter approximately 20% more than do the local pressure data set. This comparison is by no means conclusive. A similar comparison for all GPS stations and over longer time spans is necessary to evaluate the effects of smoothing in the NMC data set.

Errors in the GPS observations of station heights may also explain some of the discrepancy between the two signals. The most likely source of error in this regard would be mismodeling of the atmospheric delay caused by tropospheric water vapor. Tropospheric delay errors correlated with barometric pressure will be largely absorbed in the zenith troposphere estimates. Estimates of this error source are difficult to quantify without independent determinations of the stochastically estimated atmospheric delay parameters.

Some of the inconsistency may also arise from possible annual signatures in the GPS station height measurements which may or may not be present in the modeled estimates of the loading effects. We removed seasonal effects from the loading and GPS data sets by estimating the amplitudes and phases of an annual signal over the entire duration of both data sets. We simultaneously fit for a bias and a trend since neither data set spans an exact integer number of annual cycles. We subsequently applied the loading corrections and recomputed the variances of the residuals. Adjusting the GPS observations by the predicted loading effects reduces the variance at 10 of the 19 stations: Ny-Alesund, Tromso, Fairbanks, Yellowknife, Metsahovi, Penticton, Algonquin, Madrid, Goldstone, and JPLM. The ratio of the estimated signal power to total power in the load contributions is decreased to 63.0 ± 8.8%. Removing seasonal signals from the two time series in this way may worsen the results because seasonal variations in surface pressure are dominated by low-order spherical harmonics. The annual atmospheric loading effect may better be determined using a Love number versus a Green's function approach.

The source of the discrepancy between the predicted and the observed pressure loading signal in the GPS station heights is unclear at this time. Deficiencies in the model used to estimate the loading effects, errors in the tropospheric delay estimates used to determine the GPS vertical station positions, annual signals in either the loading estimates or the GPS measurements, or a combination of all these effects may be contributing to the difference. We suspect that the presence of significant errors in the pressure data at most sites is the most likely cause.

Correcting for Atmospheric Loading Effects

Previous investigations have demonstrated that there is a high correlation between local pressure variations and modeled surface displacement [*Manabe et al.*, 1991; *vanDam and Herring*, 1994]. *MacMillan and Gipson* [1994] go on to demonstrate that there is also a correlation between local pressure variations and VLBI-determined vertical station positions. These studies indicate that a regression between the local pressure and the modeled radial displacements or the observed vertical position changes may provide a viable means for obtaining approximate load corrections.

In Figure 5, GPS vertical station positions are plotted as a function of the deviation of the local pressure at six sites: Yellowknife (Figure 5a), Tromso (Figure 5b), Wettzell (Figure 5c), St. John's (Figure 5d), JPL (Figure 5e), and Kokee(Figure 5f). (Independent measurements of local pressure are not available for most GPS sites. "Local pressure" in this context refers to the grid value of NMC pressure that is geographically closest to the station of interest.) As expected, the correlations between the local pressure and the vertical displacements, shown in Table 5, agree closely with the correlations for the global convolution sum model, shown in Table 2.

The regression between local pressure and GPS vertical station positions for our sites (given in Table 5) exhibit slopes between -1.17 and 0.35 mm/mbar. For the six sites with slopes significantly different from zero (stations marked with a superscript f), the regression coefficient is between -0.26 and -0.59 mm/mbar. The pressure signals at these stations have signal to noise ratios greater than one (compare with Table 4). The ratios of the station height residuals to the local pressure at Ny-Alesund, Penticton, and Pinyon Flats are the same order of magnitude as their errors. The errors on the coefficients at the remaining sites are much larger than the coefficients themselves, indicating that here the coefficients are statistically consistent with zero. The coefficients presented in Table 5 are also comparable to those found by *Manabe et al.* [1991], *vanDam and*

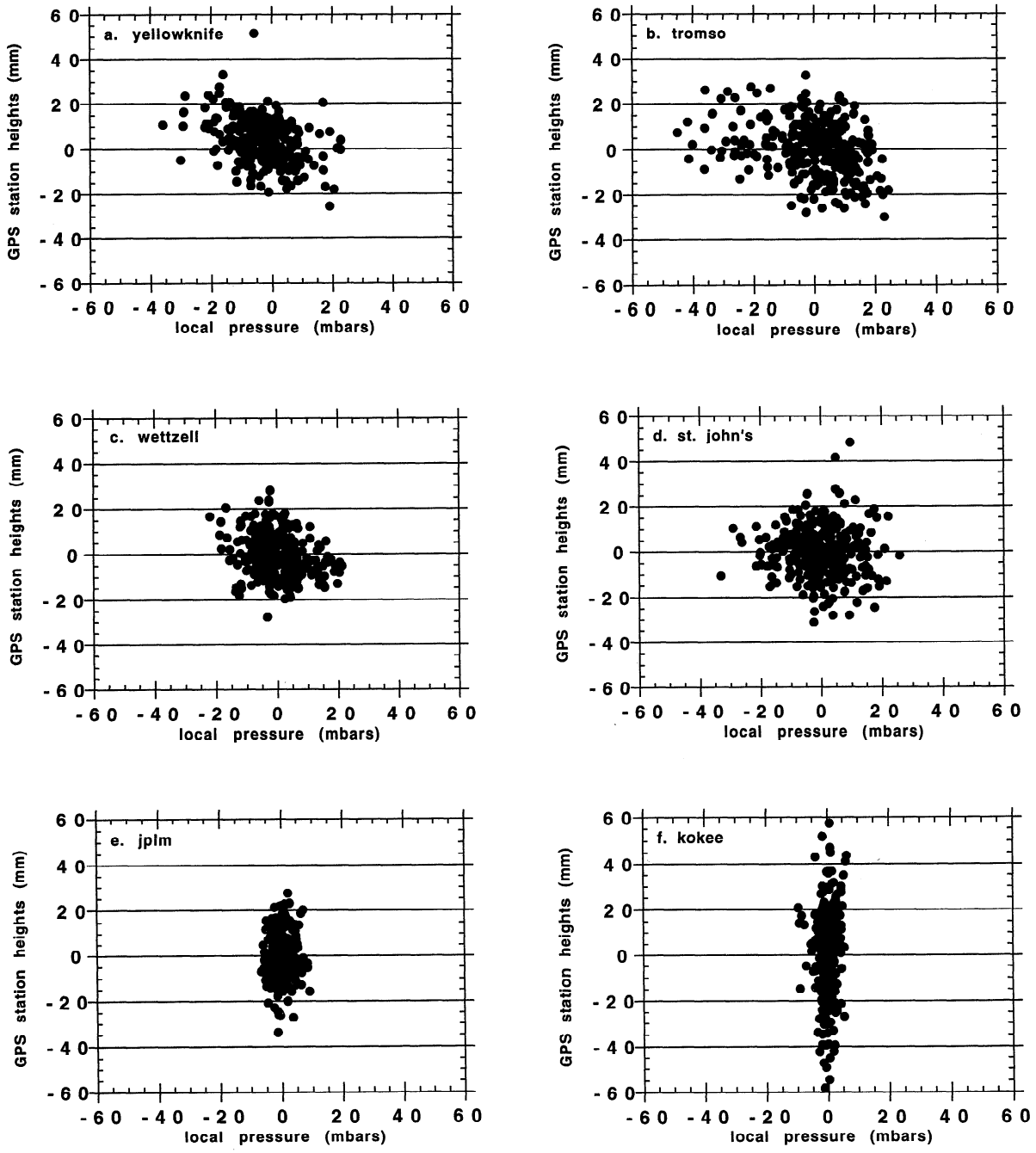

Figure 5. Scatter plots of GPS vertical displacements versus the local pressure variations at (a) Yellowknife, (b) Tromso, (c) Wettzell, (d) St. John's, (e) JPLM, and (f) Kokee.

Herring [1994] (same as model results in Table 5), and *MacMillan and Gipson* [1994].

Coefficients determined by *MacMillan and Gipson* [1994] using the same technique as above except with VLBI station heights are given in Table 5 for comparison. The VLBI coefficients more closely match the coefficients predicted by the model than the GPS results. This result may indicate that the loading signal is correlated with another signal in the GPS data that is not being removed in the GPS data processing. The coefficients determined by *Manabe et al.* [1991] are also given in Table 5. Differences between the Manabe results and the model results can be attributed to differences in the pressure fields used in determining the loading. They used surface pressures derived from the Global Objective Analysis (GANL) and obtained from the Japanese Meteorological Agency.

In correcting GPS station heights for atmospheric loading effects, the above coefficients could be used as an alternative to the global convolution sum (GCS). In Table 5, the variance

Table 5. Correlation Between Local Pressure and GPS Vertical Station Positions

Station	Correlation Coefficient, mm/mbar	Regression Coefficient, mm/mbar	Model,[a] mm/mbar	*Manabe et al.* [1991],[b] mm/mbar	VLBI,[c] mm/mbar	Variance Reduction Coefficient,[d] mm^2	Variance Reduction Model,[e] mm^2
Ny-Alesund	-0.17	-0.19 ± 0.16	-0.21 ± 0.005	----	----	-9.13 ± 6.42	-9.97 ± 6.82
Tromso[f]	-0.36	-0.31 ± 0.10	-0.29 ± 0.004	----	----	-14.94 ± 4.72	-21.54 ± 5.00
Fairbanks[f]	-0.43	-0.59 ± 0.14	-0.44 ± 0.006	-0.432	-0.35 ± 0.07	-38.86 ± 6.69	-48.95 ± 7.29
Yellowknife[f,g]	-0.37	-0.39 ± 0.13	-0.43 ± 0.005	----	----	-13.70 ± 3.36	-9.41 ± 4.04
Metsahovi[f,g]	-0.35	-0.30 ± 0.12	-0.39 ± 0.005	----	----	-11.04 ± 4.33	-8.41 ± 4.94
Onsala	0.00	0.00 ± 0.11	-0.29 ± 0.005	-0.254	-0.16 ± 0.13	11.07 ± 3.52	9.08 ± 3.92
Kootwijk[f,g]	-0.34	-0.26 ± 0.12	-0.36 ± 0.006	----	----	-4.29 ± 2.67	-0.31 ± 2.90
Herstmonceux	-0.02	-0.02 ± 0.19	-0.36 ± 0.008	----	----	7.76 ± 2.48	8.32 ± 2.69
Penticton[g]	-0.21	-0.29 ± 0.21	-0.41 ± 0.010	----	----	-2.06 ± 1.84	-1.05 ± 2.14
Wettzell[g]	-0.27	-0.30 ± 0.17	-0.43 ± 0.008	-0.442	-0.53 ± 0.80	-4.62 ± 3.07	-3.30 ± 3.32
Alberthead	-0.05	-0.08 ± 0.21	-0.29 ± 0.010	----	----	1.02 ± 1.46	2.81 ± 1.92
St. John's	-0.06	-0.06 ± 0.13	-0.20 ± 0.006	----	----	1.55 ± 2.20	2.47 ± 2.63
Algonquin[f]	-0.29	-0.35 ± 0.17	-0.37 ± 0.008	-0.435	----	-5.82 ± 2.61	-7.62 ± 2.97
Matera	-0.08	-0.12 ± 0.22	-0.35 ± 0.009	----	----	0.54 ± 2.75	2.21 ± 2.98
Madrid	-0.07	-0.15 ± 0.27	0.39 ± 0.011	----	----	1.15 ± 2.35	3.09 ± 2.68
Goldstone[f,g]	-0.24	-0.80 ± 0.47	-0.40 ± 0.019	-0.457	-0.30 ± 0.13	-5.43 ± 1.60	-3.77 ± 1.86
JPLM	0.07	0.23 ± 0.47	-0.38 ± 0.021	----	----	-0.48 ± 1.40	-0.52 ± 1.57
Pinyon Flats	-0.15	-1.17 ± 1.67	-0.36 ± 0.064	----	----	-1.96 ± 1.65	-4.55 ± 2.38
Kokee	0.05	0.35 ± 0.77	-0.11 ± 0.024	-0.053	-0.49± 0.35	0.49 ± 0.78	0.46 ± 1.44

[a]Regression between NMC pressure and local vertical displacement estimated using the global convolution sum.

[b]Regression between modeled loading effects and local pressure derived by *Manabe et al.* [1991].

[c]Regression between local pressure and VLBI measured vertical station positions [*MacMillan and Gipson*, 1994]. Blanks indicate that VLBI results are not available for these sites.

[d]This column displays the variance reduction obtained when the local regression coefficient is used to estimate the effects of atmospheric pressure loading.

[e]This column reports the variance reduction obtained when the global convolution sum is used to estimate the effects of atmospheric pressure loading.

[f]Slope deviates from zero by more than about 2 standard deviations.

[g]Stations where the regression coefficient reduced the variance of the height residuals more than the results from the global convolution sum.

reduction computed using only the local pressure is given for all sites (variance reductions computed using the GCS are presented in Table 5 for comparison). For six stations (marked with a superscript g), the regression coefficients reduce the variance of the station height residuals even more than the GCS results, indicating that there is probably another signal coherent with atmospheric pressure loading remaining in the station heights at these sites. At Ny-Alesund, Fairbanks, Algonquin, and JPLM the variance reduction is less than but still within about 30% of the reduction observed using the GCS. At these ten stations then, it is adequate to correct for atmospheric loading effects using a site dependent regression coefficient. At Pinyon Flats and Tromso on the other hand, the improvement is significantly less than that observed in the GCS case, indicating that the local pressure here is probably not very representative of the regional pressure field, and hence correcting for pressure loading using the given coefficients may underestimate the effect. Of the remaining sites, all of which still show a variance increase after applying the loading correction, only Onsala and Kokee show an even larger variance increase than in the GCS case. This result may be due to a complicated air-sea interaction at these sites, Kokee being an island in the Pacific Ocean and Onsala being situated on the narrow strait between the North and the Baltic Seas.

For sites where an improvement is observed using the GCS, using local pressure measurements alone does offer a practical solution to computing the load contribution to GPS station position measurements. With a longer time series, we may be able to compute reliable coefficients at other sites as well.

Baselines

Vertical station displacements caused by atmospheric pressure loading project into baseline length changes. Although we have already argued that this method should be less sensitive to the signal, we include the results here for completeness and as a check on the consistency with published VLBI results. In this section of the analysis, we consider all possible baselines generated by a typical global network solution (approximately 35 stations). Baseline length changes measured using GPS were compared with estimates of changes determined using the GCS. We restricted our analysis to baselines of 6000 km or longer. For baselines of this length, 50% of loading signal would project into

the length of the vector between the two endpoints. Of the 117 baselines investigated, 96 showed a reduction in baseline length scatter after the modeled effects of atmospheric pressure loading were removed. Inverting the variances demonstrates that 57 ± 0.9% of the pressure signal is evident in the baseline length residuals. Inverting the variances using data from 22 VLBI baselines, *vanDam and Herring* [1994] found that approximately 60% of the power in the load correction is signal. Hence both GPS and VLBI baseline length measurements are sensitive to atmospheric pressure loading at the same level.

Conclusions

Our analysis indicates that pressure loading contributions are clearly evident in GPS vertical station position measurements. The application of the loading corrections reduces the variance of the GPS vertical estimates by up to 24%. However, only about 65% of the computed contribution seems to be in the GPS measurements. Removing an annual signal from the loading estimates and the GPS heights does not affect this result. At this time, the origin of the additional noise in the pressure loading contribution is not clear but may be the result of a combination of effects including deficiencies in the Green's functions, inadequacies in the NMC surface pressure data, or mismodeling of the troposphere in GPS height estimates as a function of pressure. We suspect that the additional noise is most likely due to pressure errors.

The use of local pressure measurements as an alternative to the full computation of the loading contribution for predicting the effects of pressure loading at individual sites, appears to be valid at many GPS sites. However, there are sites where the effectiveness of the local regression coefficient is unreliable.

Sixty-two percent of the GPS baselines investigated in this paper show a reduction in scatter when corrected for the effects of atmospheric pressure loading. Approximately 57% of the pressure loading signal is evident in the GPS baseline length measurements, which is consistent with VLBI results.

Acknowledgments. The authors would like to thank Marshall Eubanks, Tim Dixon, and Bob King for their careful and thorough reviews. Their comments and suggestions significantly improved the quality of this paper. The authors would also like to acknowledge the assistance of Joey Comeaux and Dennis Joseph of the Data Support Group at NCAR in obtaining and interpreting the archived NMC surface pressure data. The research in this paper was conducted while T. vanDam was employed at NVI under contract NAS5-32331, by the University of Newcastle upon Tyne, and by the Jet Propulsion Laboratory, California Institute of Technology under contract with the National Aeronautics and Space Administration.

References

Blewitt, G., M.B. Heflin, F.H. Webb, U.J. Lindqwister, and R.P. Malla, Global coordinates with centimeter accuracy in the International Terrestrial Reference Frame, *Geophys. Res. Lett., 19,* 853-856, 1992.

Blewitt, G., M.B. Heflin, Y. Vigue, J.F. Zumberge, D. Jefferson, and F.H. Webb, The Earth viewed as a deforming polyhedron: Method and results, in *Proceedings of the 1993 IGS Workshop*, edited by G. Beutler and E. Brockmann, pp. 165-174, International GPS Service for Geodynamics, Bern, Switzerland, 1993.

Chelton, D.B., and D.B. Enfield, Ocean signals in tide gauge records, *J. Geophys. Res., 91*, 9081-9098, 1986.

Eubanks, T.M., Interactions between the atmosphere, oceans and crust: Possible oceanic signals in Earth rotation, in *The Orientation of the Planet Earth as Observed by Modern Space Techniques,* edited by M. Feissel, pp. 291-300, Pergamon, New York, 1993.

Farrell, W.E., Deformation of the Earth by surface loads, *Rev. Geophys., 10*, 761–797, 1972.

Heflin, M, W. Bertiger, G. Blewitt, A. Freedman, K. Hurst, S. Lichten, U. Lindqwister, Y. Vigue, F. Webb, T. Yunck, and J. Zumberge, Global geodesy using GPS without fiducial sites, *Geophys. Res. Lett., 19,* 131-134, 1992.

International Earth Rotation Service (IERS), *1992 IERS Annual Report*, Observatoire de Paris, Paris, 1993.

Lichten, S.M., and J.S. Border, Strategies for high precision Global Positioning System orbit determination, *J. Geophys. Res., 92*, 12,751-12,762, 1987.

MacMillan, D.S., and J.M. Gipson, Atmospheric pressure loading parameters from very long baseline interferometry observations, *J. Geophys. Res.*, in press 1994.

Manabe, S., T. Sato, S. Sakai, and K. Yokoyama, Atmospheric loading effect on VLBI observations, in Proceedings of the AGU Chapman Conference on Geodetic VLBI: Monitoring Global Change, *NOAA Tech. Rep., NOS 137 NGS 49*, 111-122, 1991.

Pagiatakis, S.D., The response of a realistic earth to ocean tide loading, *Geophys. J. Int., 103*, 541-560, 1990.

Rabbel, W., and J. Zschau, Static deformations and gravity changes at the Earth's surface due to atmospheric loading, *J. Geophys., 56,* 81-99, 1985.

Rabbel, W., and H. Schuh, The influence of atmospheric loading on VLBI-experiments, *J. Geophys., 59,* 164-170, 1986.

Sovers, O.J., and J.S. Border, Observation model and parameter partials for the JPL geodetic GPS modeling software "GPSOMC", *JPL Publ., 87-21, Rev.2*, 1990.

vanDam, T.M., and T.A. Herring, Detection of atmospheric pressure loading using very long baseline interferometry measurements, *J. Geophys. Res., 99*, 4505-4517, 1994.

vanDam, T.M., and J. Wahr, Displacements of the Earth's surface due to atmospheric loading: Effects on gravity and baseline measurements, *J. Geophys. Res., 92*, 1282–1286, 1987.

Vigue, Y., S.M. Lichten, G. Blewitt, M.B. Heflin, and R.P. Malla, Precise determination of the Earth's center of mass using measurements from the Global Positioning System, *Geophys. Res. Lett., 19,* 1487-1490, 1992.

Vigue, Y., S.M. Lichten, R.J. Muellerschoen, G. Blewitt, and M.B. Heflin, Improved treatment of GPS force parameters in precise orbit determination application, *Rep. Am. Astron. Soc., 93-159*, AAS Publ. Off., San Diego, Calif., 1993.

Zumberge, J.F., D.C. Jefferson, G. Blewitt, M.B. Heflin, and F.H. Webb, Jet Propulsion Laboratory IGS analysis center report, pp. 154-163, 1992, in *Proceedings of the 1993 IGS Workshop*, edited by G. Beutler and E. Brockmann, International GPS Service for Geodynamics, Bern, Switzerland, 1993.

G. Blewitt, Department of Surveying, University of Newcastle upon Tyne, Newcastle upon Tyne, NE1 7RU England. (e-mail: Geoffrey.Blewitt@newcastle.ac.uk)

M.B. Heflin, Jet Propulsion Laboratory, California Institute of Technology, 4800 Oak Grove Drive, MS 238-625 Pasadena, CA 91109. (e-mail: mbh@sideshow.jpl.nasa.gov)

T. M. vanDam, Geosciences Laboratory, NOAA/NOS/OES 13, SSMC IV, 1305 East-West Highway, Silver Spring, MD 20910. (e-mail: tonie@robeson.grdl.noaa.gov)

(Received February 2, 1994; revised August 4, 1994;
accepted August 11, 1994.)